

RESEARCH ARTICLE

Multicomponent carbohydrase system from *Trichoderma reesei*: A toolbox to address complexity of cell walls of plant substrates in animal feed

Ninfa Rangel Pedersen^{1,2}, Morten Tovborg¹, Abdoreza Soleimani Farjam³, Eduardo Antonio Della Pia^{1*}

1 Novozymes A/S Denmark, Kgs, Lyngby, Denmark, **2** Fermentationexperts A/S, Bække, Denmark, **3** Novozymes A/S Malaysia, Kuala Lumpur, Malaysia

☞ These authors contributed equally to this work.

* eap@novozymes.com



Abstract

A diverse range of monocot and dicot grains and their by-products are commonly used in the animal feed industry. They all come with complex and variable cell wall structures which in turn contribute significant fiber to the complete feed. The cell wall is a highly interconnected matrix of various polysaccharides, proteins and lignin and, as such, requires a collaborative effort of different enzymes for its degradation. In this regard, we investigated the potential of a commercial multicomponent carbohydrase product from a wild type fermentation of *Trichoderma reesei* (*T. reesei*) (RONOZYME® MultiGrain) in degrading cell wall components of wheat, barley, rye, de-oiled rice bran, sunflower, rapeseed and cassava. A total of thirty-one different enzyme proteins were identified in the *T. reesei* carbohydrase product using liquid chromatography with tandem mass spectrometry LC-MS/MS including glycosyl hydrolases and carbohydrate esterases. As measured by *in vitro* incubations and non-starch polysaccharide component analysis, and visualization by immunocytochemistry and confocal microscopy imaging of immuno-labeled samples with confocal microscopy, the carbohydrase product effectively solubilized cellulosytic and hemicellulosytic polysaccharides present in the cell walls of all the feed ingredients evaluated. The *T. reesei* fermentation also decreased viscosity of arabinoxylan, xyloglucan, galactomannan and β -glucan substrates. Combination of several debranching enzymes including arabinofuranosidase, xylosidase, α -galactosidase, acetyl xylan esterase, and 4-O-methyl-glucuronoyl methyl-esterase with both GH10 and GH11 xylanases in the carbohydrase product resulted in effective hydrolyzation of heavily branched glucuronoarabinoxylans. The different β -glucanases (both endo- β -1,3(4)-glucanase and endo- β -1,3-glucanase), cellulases and a β -glucosidase in the *T. reesei* fermentation effectively reduced polymerization of both β -glucans and cellulose polysaccharides of viscous cereals grains (wheat, barley, rye and oat). Interestingly, the secretome of *T. reesei* contained significant amounts of an exceptional direct chain-cutting enzyme from the GH74 family (Cel74A, xyloglucan-specific β -1,4-endoglucanase), that strictly cleaves the xyloglucan backbone at the substituted regions. Here, we demonstrated

OPEN ACCESS

Citation: Rangel Pedersen N, Tovborg M, Soleimani Farjam A, Della Pia EA (2021) Multicomponent carbohydrase system from *Trichoderma reesei*: A toolbox to address complexity of cell walls of plant substrates in animal feed. PLoS ONE 16(6): e0251556. <https://doi.org/10.1371/journal.pone.0251556>

Editor: Jean-Guy Berrin, INRAE, FRANCE

Received: January 26, 2021

Accepted: April 27, 2021

Published: June 4, 2021

Copyright: © 2021 Rangel Pedersen et al. This is an open access article distributed under the terms of the [Creative Commons Attribution License](https://creativecommons.org/licenses/by/4.0/), which permits unrestricted use, distribution, and reproduction in any medium, provided the original author and source are credited.

Data Availability Statement: All relevant data are within the paper and its [Supporting Information](#) files.

Funding: The author(s) received no specific funding for this work.

Competing interests: The authors have declared that no competing interests exist.

that the balance of enzymes present in the *T. reesei* secretome is capable of degrading various cell wall components in both monocot and dicot plant raw material used as animal feed.

Introduction

Modern feed industry is based on providing a precise composition of nutrients to meet specific requirements of production animals. However, in practice a degree of uncertainty remains between the formulated nutrients and the actual supplied nutrients. Such discrepancy is more prominent when it comes to non-starch polysaccharide composition. The specific structure and composition of non-starch polysaccharides in the grains not only vary by genotype, but also by the environment in which they are harvested. Plant cells dynamically remodel their cell wall structure and composition in attempt to adapt to the imposed environmental conditions [1]. Wheat grain grown under heat stress condition contain higher levels of arabinoxylan [2], and rice seedlings grown under cold stress condition contain higher levels of xyloglucan with more cross-linking to cellulose microfibrils [3, 4]. A large-scale global survey of corn, wheat and barley quality indicated 14.39, 11.23 and 15.94% variation in crude fiber content of these grains, respectively [5]. The variation may be further enhanced if the measurement is narrowed down to specific polysaccharides. The arabinoxylan (A+X) content of wheat, barley, corn, rapeseed meal and soybean meal is reported to vary by 31, 32, 50, 16 and 41%, respectively [6]. This inherent variation brings high unpredictability to the end users of these grains and their by-products. This problem becomes crucial when considering that the size of the global feed production lies at over a billion tons annually and is expected to grow 1.6 times by 2050 [7]. Traditionally, the feed industry reduces the risks associated to inherent variation of grains nutrient composition with application of exogenous cell wall degrading enzymes. Enzymatic preparations with the highest enzyme activities are therefore regarded as the best tools to ensure the consistency of nutrient supply [8]. However, learnings from nature itself point out a different way whereby cell wall polysaccharides are degraded by adopting a right set and balance of enzymatic activities. The filamentous fungus *Trichoderma reesei* (*T. reesei*) is equipped with a unique secretome that acts in synergy to degrade polysaccharides present in cell walls of both monocot and dicot grains. This includes an array of enzyme activities to hydrolyze arabinoxylan, highly branched arabinoxylan (glucuronoxylan and arabino-glucuronoxylan), β -glucan, cellulose, xyloglucan, and pectin [9, 10]. The current study was designed to characterize the secretome of a wild type fermentation from *T. reesei* and its specific enzyme activities on various feed ingredients. We have previously demonstrated the efficacy of the same carbohydrase product to hydrolyze hemicellulose components of corn substrate with inherent variations [11, 12]. Here we expand the investigation to demonstrate the activity of the *T. reesei* fermentation product on multiple monocot and dicot grains such as wheat, barley, rye, oat, rice bran, rapeseed, sunflower and cassava. The effects of the multicomponent carbohydrase product are also demonstrated by confocal microscopy visualization that allows identification of individual polysaccharides within the intact cell wall structure, by-passing the shortcomings imposed by conventional purification and hydrolysis methods.

Material and methods

Enzymes

A multicomponent carbohydrase product obtained from a fermentation of *T. reesei* (RONOZYME[®] MultiGrain (MultiGrain), DSM Nutritional Products, Basel, Switzerland) was used in

this study. The product has endo-1,4- β -glucanase (EC 3.2.1.4; 800 U/g), endo-1,3(4)- β -glucanase (EC 3.2.1.6; 700 U/g), and endo-1,4- β -xylanase (EC 3.2.1.8; 2,700 U/g) as declared activities [13] and is active within a broad pH range (4–8). The recommended dosage of MultiGrain for poultry for fattening is 100 mg product per kg feed. Amyloglucosidase (AMG) (Megazyme, Bray, Ireland) and thermostable alpha-amylase (Termamyl 300 L, Novozymes, Denmark) were used for the double destarching step of the different plant materials.

Plant material and chemicals

Whole grain wheat, barley and rye were obtained from Denmark. Oat, sunflower and rapeseed were obtained from France, de-oiled rice bran (DORB) and cassava from Thailand. All grain materials were milled to pass through a 0.5 mm sieve (ZM 200, Retsch, Haan, Germany). Rye arabinoxylan (RAX), wheat arabinoxylan (WAX), mixed linked (1–3),(1–4)- β -D-glucan (MLG), β -galactomannan and xyloglucan were purchased from Megazyme, Ireland. All other chemicals were obtained from Sigma Aldrich (St. Louis, MO, U.S.A.).

Protein identification by LC-MS/MS

Tryptic digests were prepared by a filter-aided sample preparation (FASP) method. Following digestion, the extracted peptides were analysed on a nano LC-MS/MS system: UltiMate 3000 RSLCnano / LTQ Orbitrap Velos Pro (Thermo/Dionex). For protein identification the data were searched against a specific database using the Mascot search engine (Matrix science) with Genedata Expressionist software having a 1% false discovery rate cut-off. Relative protein concentrations were calculated by label free quantification from peptide volumes using a Hi3 standard method in Genedata Expressionist.

Viscosity measurements

Solutions of RAX (1 g/100 mL), WAX (1 g/100 mL), MLG (0.5 g/100 mL), β -galactomannan (1 g/100 mL), and xyloglucan (1 g/100 mL) were prepared in 0.1 M sodium acetate buffer, pH 6 to be used as substrates. Each substrate (250 μ L) was pipetted to a 96 well microtiter plate (MTP) and incubated with 20 μ L of the carbohydrase product, or buffer (control), at 40°C for 30 mins with stirring. The final carbohydrase product was diluted to a final concentration corresponding to 9 μ g product per mL solution. Viscosity measurements were conducted using a Hamilton STARLET liquid handler (Hamilton) programmed to measure flow resistance pressure (Pa) during aspiration and dispensation as described in previous studies [14, 15].

Double destarching of substrates

Destarching was carried out as described previously [16], albeit in a much smaller scale. In short, the five milled substrates wheat, barley, rye, oat and cassava were incubated with 2% alpha-amylase (Termamyl 300 L) at 90°C for 1 hour. The reaction mixture was cooled to 40°C, 14 U/mL of AMG was then added, and the solution was incubated in a shaking water bath overnight (16 hours). The procedure was repeated and then the destarched solids were collected by centrifugation and the pellets were washed 3 times with sodium acetate buffer and freeze dried. Analysis of the resulting material indicated that more than 99% of the starch present in the grains was removed by the double destarching process.

In vitro incubations and monosaccharide analysis

To remove soluble oligomers and proteins, the milled rapeseed and sunflower samples were incubated in acetate buffer at pH 6.0 for 2 hours at 40°C. The solids were removed by

centrifugation for 15 min at 4415 g and 5°C and freeze dried. The resulting rapeseed and sunflower samples, the double destarched wheat, rye, barley oat and cassava, and rice bran were incubated (10% dry matter) with the carbohydrase product at the commercial recommended dosage in acetate buffer pH 6.0 for 2 hours at 40°C with stirring (300 rpm). Experiments were run in quadruplicates. Following incubation with the multicomponent carbohydrase product, the solids were removed by centrifugation for 15 min at 4415 g and 5°C, and 500 µL of the supernatant was subjected to acid hydrolysis (1.6 M HCl) for 1 hour at 99°C. The solution was then neutralized with 1.3 M NaOH and the resulting samples were analyzed for neutral monosaccharide contents by high performance anion exchange chromatography combined with pulsed amperometric detection (HPAEC-PAD). Separation was achieved on a CarboPac analytical PA-210 column (id 2 mm) and a CarboPac PA-210 guard column (ThermoFisher), at a temperature of 40°C with 1 mM KOH isocratic eluent flow rate of 0.2 mL/min. Seven monosaccharide standards (fucose, arabinose, rhamnose, galactose, glucose, xylose, mannose) were analyzed.

Embedding, sectioning and staining

The procedure was conducted essentially as described before [16]. Pieces of approximately 4 × 4 × 6 mm of whole rye, barley, wheat, oat, rapeseed, sunflower (containing seed coat, aleurone layer and endosperm), cassava and DORB were fixed in Karnovsky's fixative and washed in 0.1 M cacodylate buffer pH 7.3 and in demineralized water. The samples were then dehydrated in a graded series of ethanol before infiltration into melted paraplast (paraffin) at 60°C using Histochoice clearing agent (Sigma-Aldrich). Paraffin-embedded samples were sectioned into 7–10 µm thick sections on a 2030 Biocut microtome (Reichert-Jung, AU). De-paraffination was performed with Histochoice and a graded series of ethanol. Samples were stained with Calcofluor White for β-glucan and cellulose visualisation, and with Pontamine Fast Scarlet 4B for cellulose and xyloglucan visualisation.

Incubations for microscopy studies

7–10 µm thick sections of de-paraffinated whole grains and DORB were treated with Multi-Grain. 100 mg of the commercial multicomponent carbohydrase product were diluted in 5 mL 0.1 M sodium acetate buffer pH 6 containing 280 mg/L CaCl₂. 50 µL of the obtained solution was applied directly on the microscope slide of the de-paraffinated samples. The samples were incubated with the commercial multicomponent carbohydrase product for 3 hours at 25°C under slight stirring in darkness. Controls were treated with buffer without the carbohydrase product at the same conditions. After 3 hours of incubation the samples were washed gently but thoroughly with deionized water and dried at room temperature. One set of slides was used for autofluorescence analysis and others for immunolocalization.

Immunocytochemistry

Immunocytochemistry was performed on the de-paraffinated samples sections as described before [16]. Grain and antibody combinations were selected based on fit between each grain polysaccharide and the antigens used to raise the antibodies according to the manufacturer's recommendations as well as prior experience with successful fluorescence imaging (Table 1). Samples were blocked with a 5% skimmed milk solution in 1x PBS for 1 hour and washed in PBS buffer followed by incubation with appropriate rat (LM6, LM11, LM25, LM28) or mouse monoclonal antibodies ((1,3),(1,4)-β-glucan antibody). Samples were subsequently incubated with a secondary antibody (anti-rat or anti-mouse IgG) linked to an Alexa-555 fluorophore and washed in PBS buffer. Citifluor AF1 anti-fading agent (Agar Scientific, UK) was added to avoid bleaching of fluorescence signal. Minimum two separate microscope slides were

Table 1. Epitopes of commercial antibodies used in the study.

Antibody/ cat. no.	Epitope	Organism	Source
LM6	(1 → 5)- α -L-arabinan	Rat	PlantProbes (UK)
LM11	(1→4)- β -D-xylan/arabinoxylan	Rat	PlantProbes (UK)
LM25	Xyloglucan—binds to the XLLG, XXLG and XXXG oligosaccharides of xyloglucan	Rat	PlantProbes (UK)
LM28	Glucuronosyl residues in glucuroarabinoxylan	Rat	PlantProbes (UK)
400–3	(1,3),(1,4)- β -glucan	Mouse	Biosupplies Australia Pty Ltd (Australia)

<https://doi.org/10.1371/journal.pone.0251556.t001>

prepared for each specimen for both control and enzymatic treatment. A negative control was made by addition of only secondary antibody after blocking with 5% skimmed milk and washing with PBS buffer.

Confocal laser scanning microscopy imaging

The confocal microscope IX83 Confocal Laser Scanning Microscope (Olympus, Japan) equipped with the software FV31S-SW software (Olympus, Japan) was used for confocal imaging. The following excitation and emission wavelengths were used: Alexa-555 and Pontamine Fast Scarlet (ex 561 nm/em 570–620 nm), Calcofluor White and autofluorescence (ex 405 nm/em 430–470 nm). Laser intensity for Calcofluor White images was 0.03% (in contrast to 3% for autofluorescence) which ensures neglectable detection of autofluorescence signal. Optimal image settings were selected prior to the final images acquisition. Images were then adjusted for brightness and contrast using same settings for images that had to be compared.

Statistical analysis

Data analysis was performed using the software SAS JMP 15.1.0 (SAS Institute Inc., USA). Statistically significant differences were determined applying the Tukey-Kramer test at $\alpha = 0.05$, as provided in the ANOVA method in the SAS JMP statistical package.

Results

Carbohydrase product composition

Protein identification was performed on four independent production batches of MultiGrain and peptides were matched with the translated genome of *T. reesei*. The identified proteins are listed in Fig 1 with protein ID from v2.0 of the *T. reesei* database [17]. All identified carbohydrate active enzymes had identical hits in the database. More than thirty unique proteins were consistently found of which the majority were glycoside hydrolases with confirmed or predicted activity towards cell wall polysaccharides. In addition, several esterases with predicted debranching activity towards methyl and acetyl groups on hemicellulose were observed. Besides hydrolases and esterases there was a significant amount of non-hydrolytic proteins which also facilitates cell wall degradation. The most abundant ones were swollenin (ID 123992) and AA9 lytic polysaccharide monooxygenase (ID 73643). A low abundance of Chi46, a GH18 endo-N-acetyl- β -D-glucosaminidase, was also consistently found. A role of these enzymes in the modification of protein glycosylation (e.g. deglycosylation at the chitobiose core of N-glycans) has been suggested [18].

Viscosity reduction

Within 30 minutes incubation of rye and wheat arabinoxylan, β -glucan, xyloglucan and galactomannan solutions, a notable and statistically significant viscosity reduction was observed in

Class	SWISSPROT ID	Protein ID*	Function	CAZY	Short name	Reference	Substrate
Xylanases	SWISSPROT:P36217	123818	Xylanase	GH11	XYNII	[19, 20]	
	TREMBL:A0A024SDM6	121127	β-xylosidase	GH3	Xyl3A (Bx1)	[21]	
	SWISSPROT:P36218	74223	Xylanase	GH11	XYNI	[20]	
	SWISSPROT:A0A024SIB3	120229	Xylanase	GH10	XYNIII	[22]	
Debranching enzymes	SWISSPROT:Q92455	123283	Arabinofuranosidase	GH54	ABF1	[21]	
	SWISSPROT:Q99034	73632	Acetyl xylan esterase	CE5	Axe1	[23]	
	SWISSPROT:G0R6X2	54219	Acetyl xylan esterase	CE5		[24] †	
	SWISSPROT:G0RV93	123940	Glucuronoyl esterase	CE15	CIP2	[25]	
Xyloglucanase	SWISSPROT:Q7Z9M8	49081	Xyloglucanase	GH74	Cel74A	[26]	
β-glucanases	SWISSPROT:A0A024SAF4	39942	Endo-β-1,3-glucanase	GH17		[27] †	
	TREMBL:G0RU13	123726	Endo-β-1,3(4)-glucanase	GH16		[28, 29] †	
	TREMBL:G0RXH1	82633	β-1,3-glucanosyltransglycosylase	GH72		[30] †	
	TREMBL:A0A024SCX9	76672	β-glucosidase	GH3	Cel3A (Bgl1)	[31]	
Cellulose active [#]	SWISSPROT:A0A024RXP8	123989	CBH	GH7	Cel7A (Cbh1)	[32]	
	SWISSPROT:P07987	72567	CBH	GH6	Cel6A (Cbh2)	[32]	
	SWISSPROT:P07981	122081	Endoglucanase	GH7	Cel7B (Egl1)	[32, 33]	
	SWISSPROT:A0A024SH20	120312	Endoglucanase	GH5	Cel5A (Egl2)	[32, 33]	
	SWISSPROT:A0A024S2H5	123232	Endoglucanase	GH12	Cel12A (Egl3)	[33, 34]	
	SWISSPROT:P43317	49976	Glucomannanase	GH45	Cel45A (Egl5)	[34]	
Galacto(gluco)-mannan active	SWISSPROT:Q99036	56996	Endo-β-1,4-mannanase	GH5	Man5A	[35]	
	TREMBL:A0A024SGF7	72632	α-galactosidase	GH27	Ag1	[36]	
	SWISSPROT:G0RBT6						
Miscellaneous	TREMBL:A0A024RZP7	123992	Swollenin		Swollenin		
	TREMBL:A0A024SM10	73643	Lytic polysaccharide monooxygenase	AA9	AA9		
	TREMBL:A0A024SLW6		Protease				
	TREMBL:A0A024RX36		Protease				
	TREMBL:A0A024SJK4		CIP1 (cellulose induced protein)		CIP1		
	TREMBL:A0A024RZ14	124282	Glyoxal oxidase	AA5	Cro1		
	TREMBL:A0A024RVF3		CFEM domain of unknown function				
	SWISSPROT:G0RH06		Peptide inc signal				
	SWISSPROT:G0RBT6		Peptide inc signal				
	SWISSPROT:G0RQL9		CFEM domain of unknown function				

Fig 1. Proteins identified in MultiGrain grouped by enzyme class and substrate. References to characterization of the identical *T. reesei* enzyme are reported if available, otherwise reference to close fungal homologs are added to the table [19–36]. Structure diagrams are included to illustrate simplified polysaccharides commonly found in the discussed plant materials. * ID according to the discussed plant materials. † ID according to *T. reesei* database v2.0 [17], ‡ Including endoglucanase, cellobiohydrolase, and betaglucosidase, † Homolog characterized enzyme from different source.

<https://doi.org/10.1371/journal.pone.0251556.g001>

the multicomponent carbohydrase product-treated samples compared to the control samples (Table 2). These results indicated a clear degradation of viscous arabinoxylan, β-glucan, xyloglucan and galactomannan polymers. The viscosity reduction was substantial for rye and wheat arabinoxylan, β-glucan and xyloglucans, ranging from approximately 3x to 80x the reduction observed in the control samples. A lower, although still significant (P<0.05), viscosity reduction was observed for the solution containing galactomannan polymers (~2x reduction compared to the control sample).

Polysaccharide solubilization after *in vitro* incubation

The efficiency by which the multicomponent carbohydrase product could solubilize the polysaccharides of different cell walls was studied by incubating the four double destarched cereal grains (wheat, rye, barley and oat), rice bran, double destarched cassava and the two dicot grains with the carbohydrase product at the recommended commercial dosage. A significant

Table 2. Viscosity reduction of solutions of rye- and wheat-arabinoxylan, β-glucan, xyloglucan and galactomannan upon treatment with MultiGrain^(a).

Treatment	Rye arabinoxylan ^(b)	Wheat arabinoxylan	β-glucan	Xyloglucan	Galactomannan
Control	0.2 ± 0.5	3.0 ± 0.2	2.7 ± 1.4	5.3 ± 0.7	3.8 ± 0.2
MultiGrain	17.9 ± 1.1	17.1 ± 1.4	28.0 ± 1.3	13.4 ± 0.6	6.0 ± 0.5

(a) Viscosity measured as percentage change in flow resistance after 30 minutes incubation at 40 °C supplemented with a control solution (deionized water) and MultiGrain.

(b) Results given as an average and standard error of determinations made in quadruplicate.

<https://doi.org/10.1371/journal.pone.0251556.t002>

($P < 0.05$) increase in the level of soluble monomers and oligomers (measured as glucose, arabinose, xylose and galactose in the supernatant after acid hydrolysis) was observed for all grains incubated with the multicomponent carbohydrase product (Table 3). No statistically significant difference in fucose, rhamnose and mannose concentrations (data not shown) was measured when the carbohydrase product-treated cereal grains were compared to the control incubations.

Confocal microscopy imaging

Cereals. The confocal microscopy images of wheat grain cross sections are illustrated in Fig 2. Fig 2A shows a wheat sample stained with calcofluor white which selectively binds cellulose and other β -1, 4-linked glucans [37]. The cell walls of the aleurone layer were stained more intense than those in the endosperm. Following incubation with the carbohydrase product, both signals almost disappeared (Fig 2B). High presence of arabinoxylan (labelled with LM11 antibody) was detected in the cell walls of the endosperm (Fig 2C), and β -glucans in the aleurone layer (labelled with antibody against (1,3),(1,4)- β -glucans) (Fig 2E). Treatment with MultiGrain removed almost completely the epitopes recognized by both antibodies and only a low fluorescence signal was detected at the interface between the aleurone and sub-aleurone layer (Fig 2D and 2F). No fluorescence signal was detected when slides were immunolabelled with the LM28 antibody detecting branched glucuronoarabinoxylans (S1 Fig).

Cell wall structures of the pericarp, aleurone, subaleurone layers and the starchy endosperm of the barley samples were clearly detectable by Calcofluor White staining (Fig 3A). Multi-Grain treatment mostly removed the fibers in the endosperm and subaleurone layer (Fig 3B). The confocal images of barley immunolabelled with the LM28 antibody did not reveal any fluorescence signal (S2 Fig), while the ones immunolabelled with the LM11 antibody indicated variable amount of arabinoxylans (Fig 3C) [16]. Following incubation with the carbohydrase

Table 3. Arabinose, galactose, glucose and xylose measured in the acid hydrolyzed supernatant of solution of different substrates incubated with a buffer solution (control) and MultiGrain for 2 hours at 40°C^(a).

Substrate	Treatment	Arabinose ^(b)	Galactose	Glucose	Xylose
Wheat	Control	0 ± 0	1.76 ± 0.03	2.17 ± 0.30	0 ± 0
	MultiGrain	41.04 ± 0.93	2.21 ± 0.03	10.24 ± 0.56	42.54 ± 0.97
Barley	Control	0 ± 0	1.43 ± 0.05	3.59 ± 0.15	0 ± 0
	MultiGrain	14.83 ± 1.03	1.96 ± 0.21	14.79 ± 0.42	9.73 ± 0.94
Rye	Control	0 ± 0	1.28 ± 0.04	4.21 ± 0.11	0 ± 0
	MultiGrain	37.49 ± 0.89	1.81 ± 0.35	27.20 ± 0.90	38.74 ± 2.68
Oat	Control	0 ± 0	1.95 ± 0.11	1.57 ± 0.06	0 ± 0
	MultiGrain	31.08 ± 0.45	2.38 ± 0.09	9.84 ± 0.13	34.65 ± 0.32
Rice bran	Control	0.13 ± 0.01	0.13 ± 0.01	0.27 ± 0.03	0.06 ± 0.01
	MultiGrain	0.41 ± 0.01	0.20 ± 0.01	0.60 ± 0.03	0.51 ± 0.01
Rapeseed	Control	2.99 ± 0.2	2.43 ± 0.13	7.80 ± 0.16	0.40 ± 0.08
	MultiGrain	3.50 ± 0.2	2.81 ± 0.11	8.74 ± 0.2	1.26 ± 0.09
Sunflower	Control	1.22 ± 0.04	2.26 ± 0.13	5.04 ± 0.22	0.20 ± 0.05
	MultiGrain	1.47 ± 0.04	2.31 ± 0.08	5.22 ± 0.19	0.53 ± 0.06
Cassava	Control	0.16 ± 0.01	0.35 ± 0.01	0.65 ± 0.01	0.07 ± 0.01
	MultiGrain	0.26 ± 0.01	0.49 ± 0.01	0.92 ± 0.02	0.40 ± 0.01

^(a) Monosaccharides are given as mg per g of the total destarched dry matter.

^(b) Results given as an average and standard error of determinations made in quadruplicate.

<https://doi.org/10.1371/journal.pone.0251556.t003>

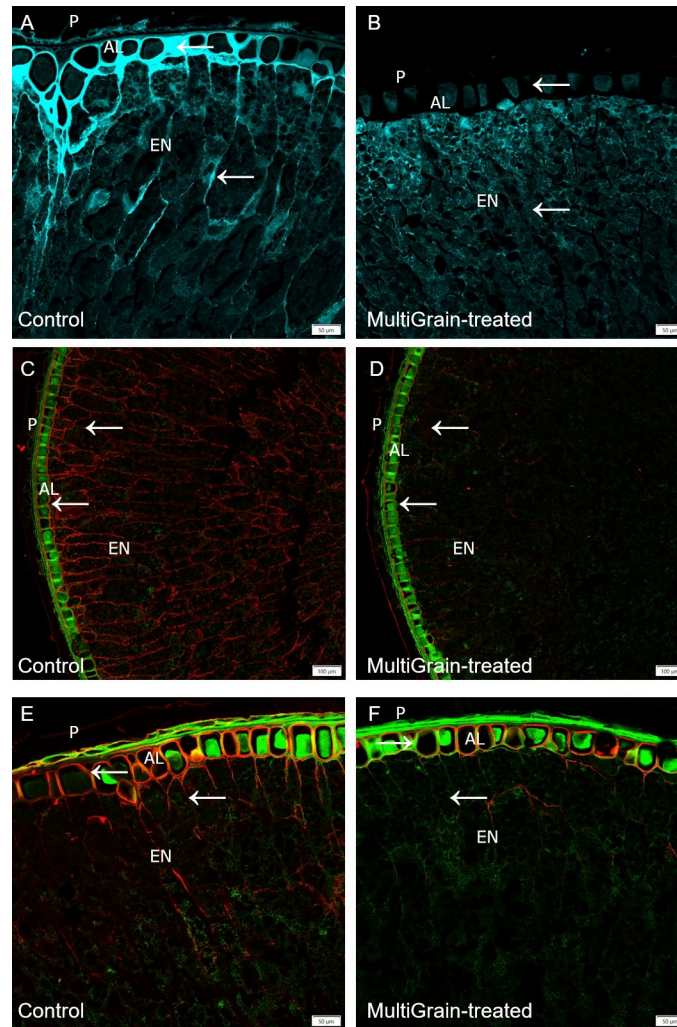


Fig 2. Confocal images of cross sections of whole wheat grains. Section of samples incubated (A, C, E) with sodium acetate buffer (control) or (B, D, F) with MultiGrain for 3 hours at pH 5. The sections were subsequently (A, B) stained with Calcofluor White, or (C, D) incubated with the LM11 antibody detecting arabinoxylans with low degree of branching and the red-fluorescence labelled secondary antibody, or (E, F) incubated with the antibody detecting (1,3), (1,4)- β -glucan and the red-fluorescence labelled secondary antibody. (A, B) Light blue signal indicates cellulose and other β -1,4-linked glucans. Red signal indicates (C, D) arabinoxylans and (E, F) β -glucans and green signal indicates autofluorescence. P = pericarp; AL = aleurone; EN = starchy endosperm. Arrows point to sites where the fluorescence signal due to staining or immunolabelling is present and removed following treatment with MultiGrain. (A, B) Scale bar = 50 μ m, (C, D) Scale bar = 100 μ m, (E, F) Scale bar = 50 μ m.

<https://doi.org/10.1371/journal.pone.0251556.g002>

product, the arabinoxylan structures almost disappeared (Fig 3D). Abundant presence of β -glucans was detected in the cell walls of the endosperm (Fig 3E). These structures disappeared completely upon incubation with the carbohydrase product (Fig 3F).

Aleurone layer and endosperm cell walls of rye grains stained intensely with Calcofluor White (Fig 4A). Carbohydrase product treatment of the sections removed stainable material from the starchy endosperm cell walls completely (Fig 4B). Staining samples with Pontamine Fast Scarlet, a dye that fluoresces preferentially in the presence of cellulose and xyloglucan [38, 39], resulted in a strong fluorescence signal from the endosperm cell walls (Fig 4C). Upon incubation with the multicomponent carbohydrase product, the fluorescence signal completely disappeared (Fig 4D). While the LM11 and β -glucan antibodies bound to the cell

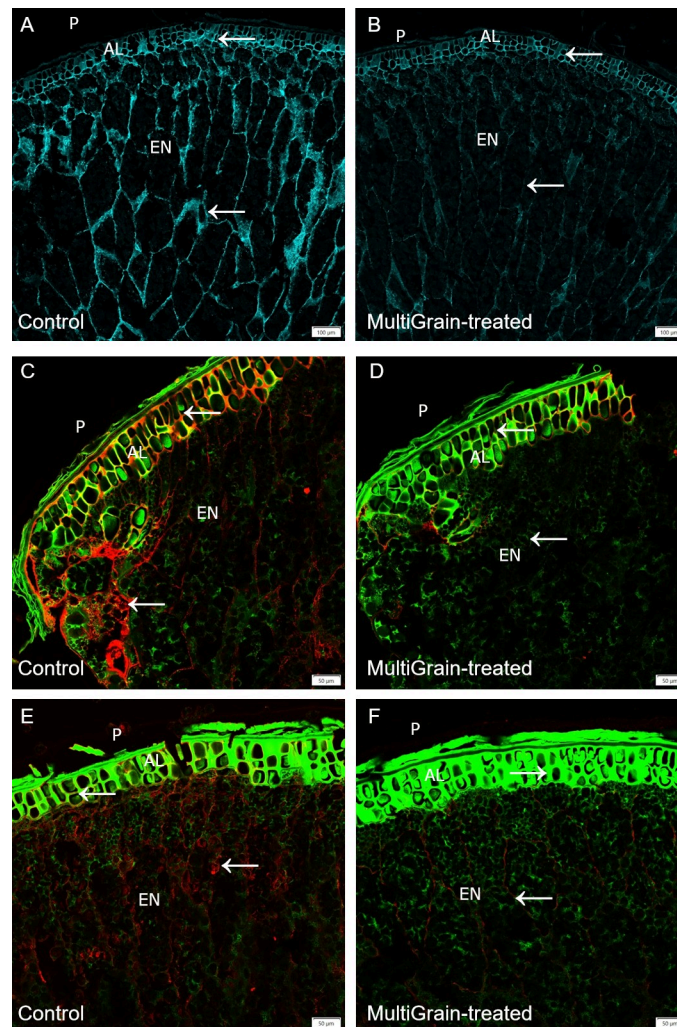


Fig 3. Confocal images of cross sections of whole barley grains. Section of samples incubated (A, C, E) with sodium acetate buffer (control) or (B, D, F) with MultiGrain for 3 hours at pH 5. The sections were subsequently (A, B) stained with Calcofluor White, or (C, D) incubated with the LM11 antibody detecting arabinoxylans with low degree of branching and the red-fluorescence labelled secondary antibody, or (E, F) incubated with the antibody detecting (1,3), (1,4)- β -glucan and the red-fluorescence labelled secondary antibody. (A, B) Light blue signal indicates cellulose and other β -1,4-linked glucans. Red signal indicates (C, D) arabinoxylans, (E, F) β -glucans and the green signal indicates autofluorescence. P = pericarp; AL = aleurone; EN = starchy endosperm. Arrows point to sites where the fluorescence signal due to staining or immunolabelling is present and removed following treatment with MultiGrain. (A, B) Scale bar = 100 μ m. (C-F) Scale bar = 50 μ m.

<https://doi.org/10.1371/journal.pone.0251556.g003>

walls of the starchy endosperm and aleurone layer (Fig 4E and 4G, respectively), the LM28 antibody bound only to the cell walls in the germ (Fig 4I). Following incubation with the carbohydrase product the fluorescence signal disappeared and only a low fluorescence signal was measured in the sub-aleurone layer or throughout the endosperm (Fig 4F, 4H and 4J).

Both the cell walls of the endosperm and aleurone layer of the oat grain were clearly stained with Calcofluor White (Figs 5A and S3A). The fluorescence signal was removed completely in the endosperm and partly in the aleurone layer after treatment with the carbohydrase product (Figs 5B and S3B). β -glucans presence in oat was mostly evident in the pericarp and endosperm (Figs 5C and S4A). Treatment with the multicomponent carbohydrase product removed completely the epitopes recognized by the anti- β -glucan antibody (Figs 5D and S4B).

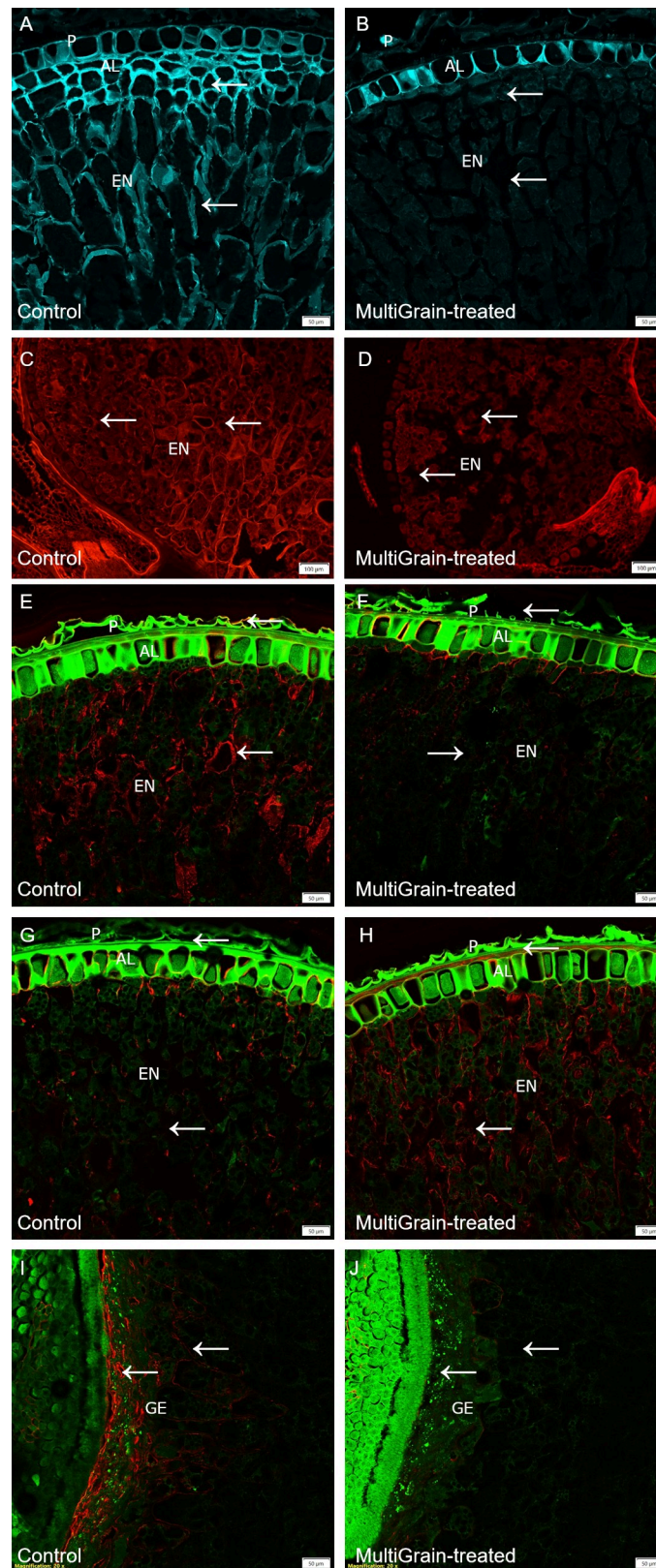


Fig 4. Confocal images of cross sections of whole rye grains. Section of samples incubated (A, C, E, G, I) with sodium acetate buffer (control) or (B, D, F, H, J) with MultiGrain for 3 hours at pH 5. The sections were subsequently

(A, B) stained with Calcofluor White, or (C, D) stained with Pontamine Fast Scarlet, or (E, F) incubated with the LM11 antibody detecting arabinoxylans with low degree of branching and the red-fluorescence labelled secondary antibody, or (G, H) incubated with the antibody detecting (1,3),(1,4)- β -glucan and the red-fluorescence labelled secondary antibody, or (I, J) incubated with the LM28 antibody detecting glucuronoarabinoxylan with high degree of branching and the red-fluorescence labelled secondary antibody. (A, B) Light blue signal indicates cellulose and other β -1,4-linked glucans. Red signal indicates (C, D) cellulose structures, (E, F) arabinoxylans, (G, H) β -glucans, (I, J) glucuronoarabinoxylans and the green signal indicates autofluorescence. P = pericarp; AL = aleurone; EN = starchy endosperm, GE = germ. Arrows point to sites where the fluorescence signal due to staining or immunolabelling is present and removed following treatment with MultiGrain. (A-D) Scale bar = 100 μ m. (E-J) Scale bar = 50 μ m.

<https://doi.org/10.1371/journal.pone.0251556.g004>

Industrial thermal and mechanical pretreatment of whole rice to obtain the DORB samples results in a very complex cell wall structure. The microscopy pictures reported in Fig 6 are representative of several analyzed samples. Imaging of the DORB samples showed that while processing destroyed most of the starchy endosperm cell wall structure, the rice pericarp and aleurone layer were resistant to the processing method (Fig 6A and 6C). The DORB samples showed high auto-fluorescence signal most likely due to the high content of ferulic acid in the outer cell wall structure (Fig 6A and 6C) [40]. Intensity of the autofluorescence signal decreased after carbohydrase product treatment (Fig 6B and 6D). Immunolabelling with LM28 and LM25 antibodies showed that complex glucuronoarabinoxylans and xyloglucans were present in the samples (Fig 6A and 6C, respectively). Neither of the fluorescence signals were detectable upon incubation with the carbohydrase product (Fig 6B and 6D). No arabinoxylans with low degree of branching were detected in the samples as visualized by incubation with LM11 antibody immunolabelling (S5 Fig).

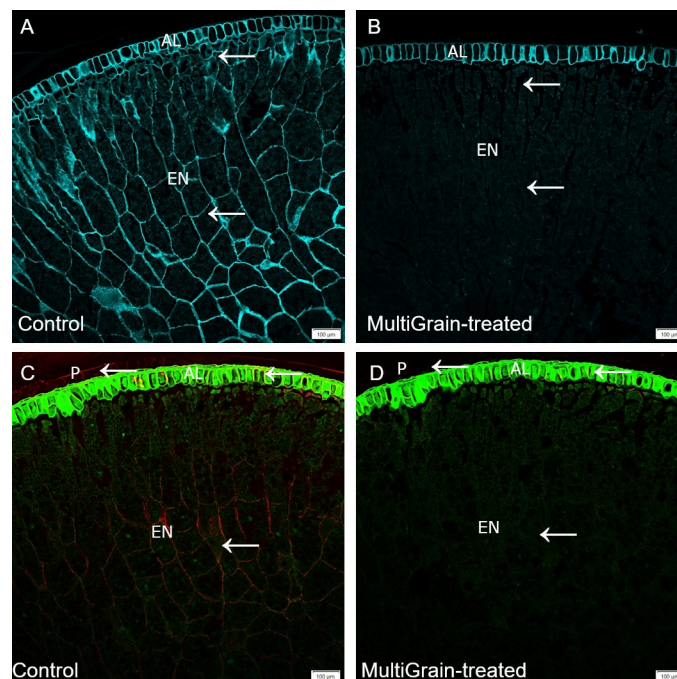


Fig 5. Confocal images of cross sections of whole oat grains. Section of samples incubated (A, C) with sodium acetate buffer (control) or (B, D) with MultiGrain for 3 hours at pH 5. The sections were subsequently (A, B) stained with Calcofluor White, or (C, D) incubated with the antibody detecting (1,3),(1,4)- β -glucan and the red-fluorescence labelled secondary antibody. (A, B) Light blue signal indicates cellulose and other β -1,4-linked glucans. Red signal indicates (C, D) β -glucans and the green signal indicates autofluorescence. AL = aleurone; EN = starchy endosperm. Arrows point to sites where the fluorescence signal due to staining or immunolabelling is present and removed following treatment with MultiGrain. (A, B) Scale bar = 100 μ m. (C, D) Scale bar = 50 μ m.

<https://doi.org/10.1371/journal.pone.0251556.g005>

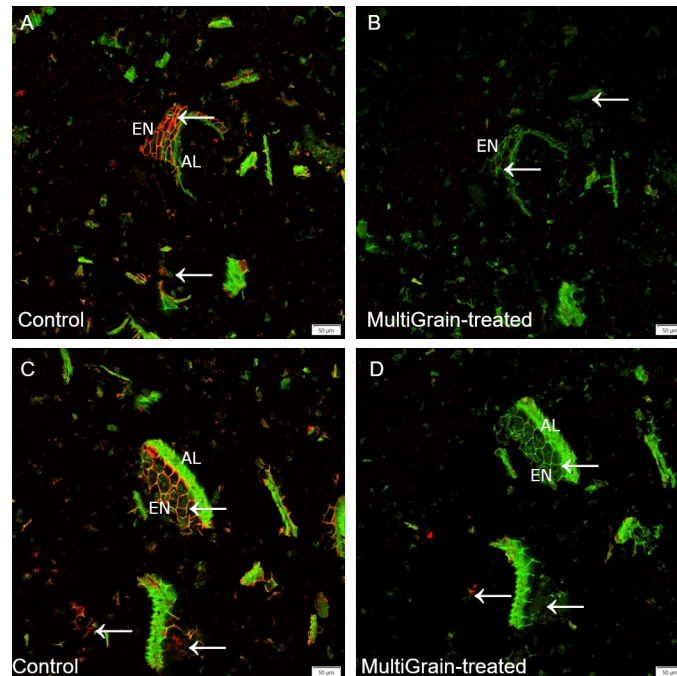


Fig 6. Confocal images of cross sections of DORB. Section of samples incubated (A, C) with sodium acetate buffer (control) or (B, D) with MultiGrain for 3 hours at pH 5. The sections were subsequently (A, B) incubated with the LM28 antibody detecting arabinoxylans and the red-fluorescence labelled secondary antibody or (C, D) incubated with the LM25 antibody detecting xyloglucans with different branching structures and the red-fluorescence labelled secondary antibody. Red signal indicates (A, B) glucuronoarabinoxylans and (C, D) xyloglucans and the green signal indicates autofluorescence. AL = aleurone; EN = starchy endosperm. Arrows point to sites where the fluorescence signal due to staining or immunolabelling is present and removed following treatment with MultiGrain. (A-D) Scale bar = 50 μ m.

<https://doi.org/10.1371/journal.pone.0251556.g006>

Dicotyledons. Confocal images of rapeseed sections immunolabelled with LM25 and LM6 antibodies are illustrated in Fig 7A and 7C, respectively. The immunolabelling fluorescence signal due to binding of the LM25 antibodies that recognize different substituted epitopes in highly branched xyloglucan was very intense and homogeneous in the cotyledon cell walls (Figs 7A and S6A). The fluorescence signal due to the immunofluorescent probe LM6 detecting (1–5)- α -L-arabinans however was mostly concentrated in the seed coat with minor presence in the cell walls of the cotyledon (Fig 7C). Upon incubation with the carbohydrase product the fluorescence signal notably reduced in intensity indicating removal of the epitopes recognized by both the LM25 and LM6 antibodies (Figs 7B and 7D and S6B and S7). The micrographs of rapeseed show autofluorescence from protein bodies within the cell walls upon UV-excitation (coloured in green in Fig 7A and 7C). Following incubation with MultiGrain, the autofluorescence signal of the protein bodies decreased in intensity and became less homogeneous (Fig 7B and 7D).

The presence of xyloglucans and (1–5)- α -L-arabinans in sunflower seed cross sections was visualised by immunolabelling with antibodies LM25 and LM6, respectively (Fig 8A and 8C). Both the antibodies bound homogeneously to the cell wall structures in the cotyledon (Fig 8A and 8C). After incubation with the carbohydrase product, the xyloglucans signal completely disappeared (Fig 8B), while a decrease in arabinan signal was observed (Fig 8D).

The presence of xyloglucans in cassava root cross sections was visualised by immunolabelling with antibodies LM25 (Fig 9). The antibodies bound homogeneously to the cell wall structures in the tuberous root (Fig 9A). Following incubation with MultiGrain, the xyloglucans

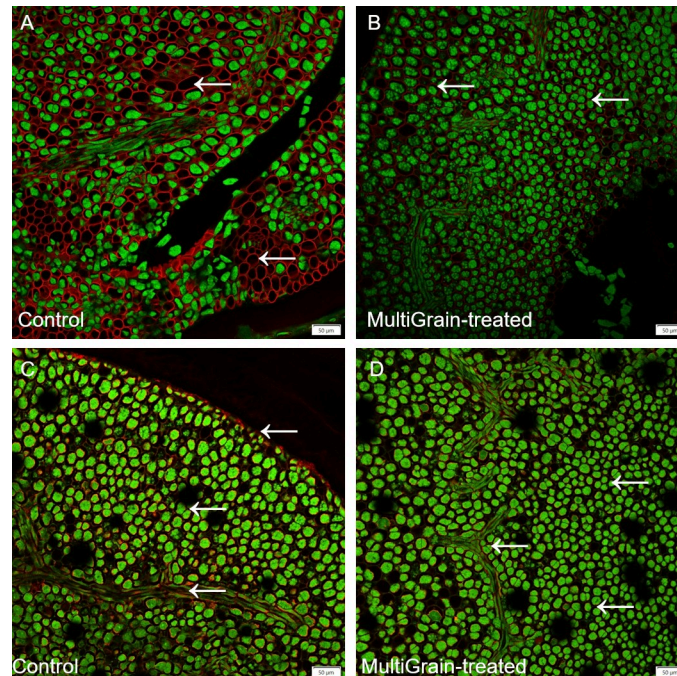


Fig 7. Confocal images of cross sections of whole rapeseed seeds. Sections of sample incubated (A, C) with sodium acetate buffer (control) or (B, D) with MultiGrain for 3 hours at pH 5. Slides were subsequently incubated with (A, B) the LM25 antibody detecting xyloglucans or (C, D) with the LM6 antibody detecting (1-5)- α -L-arabinans. Red fluorescence labelled secondary antibody used for visualization of sections. Red signal indicates (A, B) xyloglucans or (C, D) arabinans and the green signal indicates autofluorescence from proteins bodies. Arrows point to sites where the fluorescence signal due to staining or immunolabelling is present and removed following treatment with MultiGrain. Scale bar = 50 μ m.

<https://doi.org/10.1371/journal.pone.0251556.g007>

signal decreased in intensity (Fig 9B). No fluorescence signal was detected when slides were immunolabelled with the LM6 antibody detecting (1-5)- α -L-arabinans (S8 Fig).

Discussion

Plant cell walls have complex structures that differ significantly across species and botanic structures. Furthermore, different cell types in the same species have unique cell walls that differ in content and composition of their polysaccharide components. The insoluble and tightly packed nature of the cell wall fibers severely limits access to nutrients such as starch and protein by the primary endogenous enzymes during gastrointestinal passage. *T. reesei* is a common filamentous aerobic fungus used for industrial applications [10]. It is well known for its great potential for enzyme production and its genome contains a wealth of genes coding for cell wall-degrading enzymes [10, 41]. Protein identification of MultiGrain, a specific commercial multicomponent carbohydrase preparation of *T. reesei*, revealed thirty-one unique proteins (Fig 1), many of which correspond to previous reports of *T. reesei* proteomics [10, 42, 43]. Most of the identified proteins are glycosyl hydrolases and carbohydrate esterases with predicted activity on cell wall polysaccharides.

A total of four xylanases were identified. The neutral pH optimum GH11 xylanase XYNII [19] was the dominating xylanase in the *T. Reesei* fermentation and it was complemented with the neutral GH10 xylanase XYNIII [22] and the more acidic GH11 xylanase XYNI [20]. Another xylanase XYNIV was shown to have both endo- and exo- activities on arabinoxytan and glucuronoarabinoxytan [44]. Two other enzymes belonging to the xylan-degrading

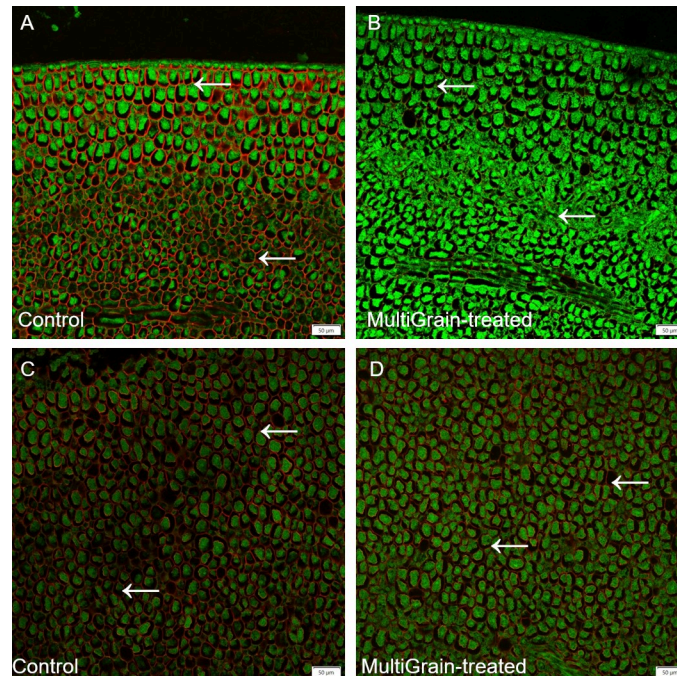


Fig 8. Confocal images of cross sections of whole sunflower seeds. Sections of sample incubated (A, C) with sodium acetate buffer (control) or (B, D) with MultiGrain for 3 hours at pH 5. Slides were subsequently incubated (A, B) with the LM25 antibody detecting xyloglucans with different branching structures or (C, D) with the antibody detecting (1–5)- α -L-arabinans. Red fluorescence labelled secondary antibody used for visualization of sections. Red signal indicates (A, B) xyloglucans having highly branched substitutions or (C, D) (1–5)- α -L-arabinans and the green signal indicates autofluorescence from proteins bodies. Arrows point to sites where the fluorescence signal due to staining or immunolabelling is present and removed following treatment with MultiGrain. Scale bar = 50 μ m.

<https://doi.org/10.1371/journal.pone.0251556.g008>

enzymes group were also identified; a beta-xylosidase (Xyl3A) and an arabinoxylan-debranching enzyme arabinofuranosidase (ABFI), the latter of which cleaves off arabinofuranosyl substitutions improving the xylan backbone accessibility to GH10 and GH11 xylanases [21]. Three carbohydrate esterases were identified. CIP2 is a CE15 enzyme specific for hydrolyzing ester linkages between alcohol groups in lignin and the acid of methyl-glucuronoyl group in

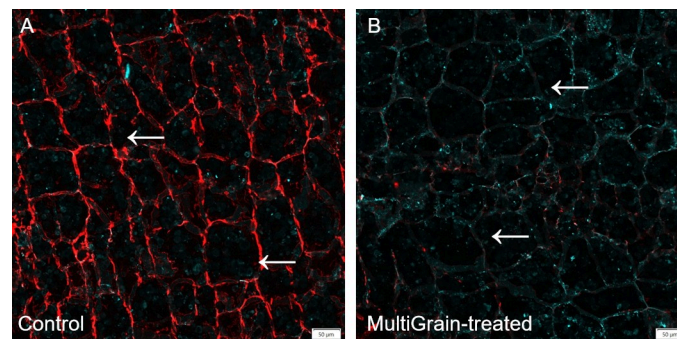


Fig 9. Confocal images of cross sections of whole cassava root. Sections of sample incubated with (A) sodium acetate buffer (control) or (B) with MultiGrain for 3 hours at pH 5. Slides were subsequently incubated with the LM25 antibody detecting xyloglucans and the red fluorescence labelled secondary antibody. Red signal indicates xyloglucans with different branching structures and the blue signal indicates autofluorescence from cell walls structures. Arrows point to sites where the fluorescence signal due to staining or immunolabelling is present and removed following treatment with MultiGrain. Scale bar = 50 μ m.

<https://doi.org/10.1371/journal.pone.0251556.g009>

glucuronoxylan [25, 45]. The CE15 glucuronoyl esterase is therefore responsible for detaching glucuronoxylan from lignin and hence making the polysaccharide more available for carbohydrases. One of the two CE5 acetyl xylan esterases (Axe1) has been confirmed to have acetyl xylan esterase activity [23]. Incubation of the *T. reesei* carbohydrase product with four cereal grains (wheat, barley, rye and oat) confirmed that the xylanases were active on different feed raw materials. In fact, neutral monosaccharide analysis of the acid hydrolyzed solubilized fraction of untreated and MultiGrain-treated samples indicated that arabinoxylans were hydrolyzed into soluble monomers and oligomers (Table 3). Interestingly, galactose was also identified in the neutral monosaccharide analysis of all the MultiGrain-treated samples. This could indicate that galactose was also present on the side chains of the solubilized arabinoxylan oligomers. The confocal microscopy pictures also demonstrated how MultiGrain could hydrolyze both low and highly-substituted arabinoxylans (Figs 2C, 2D, 3C, 3D, 4E, 4F, 6A and 6B). Hydrolysis of different arabinoxylan structures by the multicomponent carbohydrase was clearly confirmed by the immunolabelling of the cereals cell walls and subsequent confocal microscopy analysis. Presence of the beta-xylosidase, the arabinofuranosidase, the GH27 alpha-galactosidase and the three carbohydrate esterases in the carbohydrase product is fundamental to cleave the highly substituted arabinoxylans like the ones present in rice bran (Fig 6A and 6B) and rye (Fig 4I and 4J). In fact, these glycosyl hydrolases and esterases act synergistically with the xylanases by cleaving arabinose, xylose, galactose, acetyl groups and the other substituents from the xylan backbone and leaving it accessible to the GH10 and GH11 xylanases. The current study clearly demonstrated that the carbohydrase product from *T. reesei* could hydrolyze arabinoxylans with different levels of substitution into oligomers such as arabinoxylo-oligosaccharides (AXOS). Recent work in our laboratory showed that combination of a xylanase and an α -arabinofuranosidase can effectively solubilize complex glucuronoarabinoxylans into AXOS [46]. Oligomers such as AXOS and XOS are generally known to have prebiotic effects enhancing gut functionality, feed conversion ratio and body weight gain [45–47].

Soluble arabinoxylans are known to bind water leading to high viscosity of the intestinal content, reducing both nutrients digestion and feed intake capacity while increasing intestinal inflammation [47, 48]. Xylanase-based products are commonly used in the feed industry to reduce the antinutritional effects of arabinoxylans. It is widely recognized that these carbohydrases exert in part their beneficial effects by reducing the viscosity of the intestinal content [49, 50]. Viscosity measurements of extracted soluble arabinoxylans incubated in presence of MultiGrain (Table 2) clearly demonstrated that the xylanases of the multicomponent carbohydrase product were effective in depolymerizing soluble arabinoxylans from both wheat and rye.

Mixed linked (1→3), (1→4)- β -D-glucans (β -glucans) represent the second most abundant non-starch polysaccharides fraction in wheat, barley, rye and oat [51]. Three enzymes with specific activity on β -glucan were identified in MultiGrain (Fig 1). They belong to families GH16, GH17, and GH72, and have different mechanisms in their β -glucan hydrolysis. The GH17 and GH72 enzymes both hydrolyze internal β -1,3-linkages. In the hydrolysis process the GH17 introduces short terminal β -1,6 branches on the glucan [27] and the GH72 elongates another β -glucan on the non-reducing end [30]. The endo- β -1,3(4)-glucanase from GH16 was shown to degrade mixed linkage β -glucan from barley by specifically hydrolyzing internal β -1,3 linkage [28, 29]. There were also three endoglucanases (Cel5A, Cel7B, cel12A) and a β -glucosidase Cel3A in the *T. reesei* fermentation that have β -glucanase activity, in addition to activity on glucomannan which complement the glucomannanase Cel45A [34]. The immunofluorescence microscopy experiments confirmed that *T. reesei* carbohydrase product removed β -glucan epitopes [52] from both the aleurone and endosperm cell structures of wheat (Fig 2E and 2F), barley (Fig 3E and 3F), rye (Fig 4G and 4H) and oat (Fig 5C and 5D). A

high degree of solubilization of β -glucans was also confirmed by the results of the *in vitro* incubations of the four destarched cereal grains (Table 3). The acid hydrolyzed solubilized fraction of the samples treated with MultiGrain showed five to six times more glucose than control samples. Barley and oat have high levels of viscous soluble β -glucans [50] that most likely cause decrease in animal performance. Several researchers have described the negative effects of soluble β -glucans in barley and demonstrated that the addition of β -glucanase to broilers diets can ameliorate the viscosity problems associated with barley [53]. Addition of MultiGrain to soluble β -glucans solutions clearly demonstrated that the different β -glucanases present in the *T. reesei* carbohydrase product effectively reduced the viscosity of the soluble pentosans medium by shortening soluble β -glucan chains (Table 2). Our observations support the findings of Brenes *et al.* that demonstrated that addition of MultiGrain to highly viscous barley-based diets significantly improves broilers performance parameters and reduces the size of the pancreas and of the gastrointestinal tract [54].

Several enzymes directly active in cellulose degradation were identified in the *T. reesei* carbohydrase product. These were the cellobiohydrolases CBH1 (Cel7A) and CBH2 (Cel6A), the endoglucanases (Cel7B, Cel5A, Cel12A), and the β -glucosidase (Cel3A). All of these play a role in degrading crystalline and amorphous cellulose [31, 32, 34]. Lytic polysaccharide monoxygenase (LPMO) (AA9) is also present. The LPMO from family AA9 has a key role in lignocellulose degradation. Even though the LPMO would be predicted to have little impact in the largely anaerobic intestinal environment, recent studies have shown that H_2O_2 can replace O_2 for LPMOs to break the glycosidic bonds [55]. In this study we used Calcofluor White to stain cellulose in selected cereal grains as seen in Fig 2 (wheat), Fig 3 (barley), Fig 4 (rye), and Fig 5 (oat). Calcofluor White also stains other β -1,4-glucan structures such as cellulose and callose. In all the examples above we observed Calcofluor White signal both in endosperm and aleurone cell walls, but in general the signal is stronger in the aleurone layer. Although cellulose is more abundant in the outer seed coat, it is also present in the aleurone cell wall [37]. In all four cereals, incubation with the carbohydrase product significantly reduced the fluorescence signal. In the aleurone layer there was a strong reduction in fluorescence signal suggesting degradation of cellulose and β -glucan structures. In the endosperm, where the signal was most likely from β -glucan, the fluorescence signal was almost complete lost. The cell walls in the aleurone cells appeared to differ in resistance to degradation by the carbohydrase product most likely due to differences in β -glucan branched structure. In the wheat sample the signal was completely lost, whereas the aleurone cell walls were still visible in the remaining cereals. Part of the lignocellulosic pericarp in rye was visible on the outside of the aleurone layer stained with Pontamine Fast Scarlet (Fig 4C). In the sample treated with MultiGrain not only were the cell walls of the endosperm missing, but most of the pericarp was either degraded or detached and lost resulting in full exposure of the nutrient rich aleurone cells.

GH54 arabinofuranosidases are α -1,5-acting and typically ascribed the function of removing α -1,5-linked arabinosyl branches in arabinoxylan as described above. However, they are not necessarily specific for this single monosaccharide branch and are also capable of hydrolyzing arabinan in pectic structures e.g. found in oil seeds such as rapeseed, sunflower and soybean. The linear arabinan is largely an α -1,5-homopolymer of arabinofuranose. Arabinofuranosidases closely related to *T. reesei* GH54 readily release arabinose from arabinan [56]. The LM6 antibody is specific for α -1,5-arabinan [57] and thus labelled the α -1,5-arabinan branches attached to pectin (rhamnogalacturonan I) present in cotyledon cell walls of rapeseed (Fig 7C) and sunflower seeds (Fig 8C). These signals faded away after incubation with MultiGrain (Figs 7D and 8D), indicating that most of the recognized antigen was degraded. Hence, the arabinofuranosidase found in the carbohydrase product was capable of reducing the arabinose branches of pectin to a high degree [58], but possibly left behind stumps of arabinan

branches on the pectic backbone. The activity of the arabinofuranosidase was also confirmed by the results of the *in vitro* incubations of the rapeseed and sunflower samples (Table 3). The acid hydrolyzed solubilized fraction of the samples treated with MultiGrain showed more arabinose than control samples. The activity of the arabinofuranosidase on arabinogalactanans present in cereal cell walls could also explain the galactose measured in the acid hydrolyzed solubilized fraction of the cereal samples treated with MultiGrain.

Xyloglucan is the main hemicellulosic polysaccharide component of primary cell wall in dicotyledonous plant seeds, while mixed linked β -1,3(4)-glucanase and arabinoxylans are the predominant hemicelluloses in cereal grains [59, 60]. Immunocytochemistry visualization confirmed abundant presence of xyloglucan in DORB (Fig 6A), rapeseed (Fig 7A) sunflower (Fig 8A) and cassava (Fig 9A). Xyloglucans have been reported to be important component of cell wall structure in soybean, rapeseed, sunflower, cassava and other legumes commonly used as feedstuff [14, 61, 62]. Xyloglucans have α -1,4-linked glucosyl backbone that is heavily substituted by α -(1,6)-D-xylosyl residues. Generally, one in every four glucose units is left unsubstituted forming repeating (XXXG)_n. The complexity of secondary substitution with other saccharides such as galactose, xylose, arabinofuranose, galacturonic acid and fucose varies and depends on the plant genotype and environmental factors [63]. Therefore, efficient degradation of xyloglucan structures requires synergistic action of both main chain and side chain enzymes. Common fungal secretomes such as *T. reesei*, *Aspergillus spp.*, *Penicillium spp.* have such combination of activities, but with some major differences. While the secretome from *A. niger* and *P. oxalicum* have more arabinofuranosidases as debranching enzyme, those from *T. reesei* have higher level of esterases for the same function [9] (Fig 1). Moreover, *T. reesei* and *A. niger* secretomes have one xyloglucan-specific β -1,4-endoglucanase belonging to the GH74 and GH12 families, respectively (Fig 1), while *P. oxalicum* secretome has no specific xyloglucan backbone degrading enzymes [9]. It is noteworthy to mention that many xyloglucan hydrolases have minor endo-1,4- β -D-glucanase (EG) activity, and many EGs have minor xyloglucan-hydrolyzing activity. However, the xyloglucanase (Cel74A) from *T. reesei* secretome is an exception as it acts on substituted motif on xyloglucan backbone [64, 65] and therefore has no activity on carboxymethylcellulose (CMC) and barley β -glucan [26]. This is possible because the Cel74A enzyme has a groove shape in the active site that allows for accommodation of the bulky side chains of xyloglucan polysaccharide [64, 66]. The direct chain-cutting Cel74A from *T. reesei* is an endo-processive enzyme with regio-specificity on substituted backbone motifs. The enzyme acts initially on the internal bond of the substrate and then acts on the same substrate as an exo-enzyme, cleaving disaccharide residues. Based on the observations in the current study and regardless of the substrate sources, the final degradation of xyloglucan by Cel74A was very extensive (Figs 6B, 7B and 8B and Table 3). Such degradation showed to produce oligosaccharides and disaccharides [65] with potential prebiotic functionality, while dismantling the cell wall structure and decreasing viscosity (Table 2). Supplementation of MultiGrain to diets with sunflower meal (SFM) resulted in better performance in broiler chickens [67]. In the study, digestibility of the hemicellulose fraction of diets with 8 and 16% SFM was markedly enhanced (37 vs 54% and 15 vs 45%, respectively) by supplementation of the multicomponent carbohydrase product from *T. reesei*. In a different study a similar enzyme treatment resulted in improvement of weight gain and feed efficiency in broiler chickens fed diets with 10 and 20% rice bran inclusion [68].

Galactomannan polymers (galactose branched β -mannan backbone) are only found in low levels in common monogastric diets. Soybean meal (SBM) from dehulled soy contain a low level of galactomannan but consistently above 1% (1.26 ± 0.14 n = 14) where the average galactose branching is 50% [69]. Less common raw materials such as palm kernel meal and copra meal have significantly higher galactomannan content with lower branching and hence

solubility. The *T. reesei* secretome contained two enzymes characterized as mannanases (Fig 1). The first, Cel45A, has activity towards cellulose as well as high activity towards glucomannan (unbranched konjac glucomannan with 40% glucose) suggesting the enzyme cleaves at β -1,4-glucose residues [34]. Among the original *T. reesei* classified endoglucanases, Cel45A was the one with highest activity on glucomannan. The second mannanase, Man5A, selectively cleaves at the β -1,4-mannose residues, which allows for degradation of galactomannan having mannan backbone as shown in work conducted with locust bean gum [35, 70]. In this case the products were manno-oligosaccharides with galactose branches. The significant reduction in galactomannan viscosity shown could be directly linked to this mannanase (Man5A). The galactose branches in galactomannan are targeted by certain GH27 enzymes. The *T. reesei* alpha-galactosidase (GH27 Ag11) was shown to contribute to galactomannan degradation by removing α -1,6 linked galactose branches [36]. The three endoglucanases (Cel5A, Cel7B, Cel12A) have all also been reported to have some activity on glucomannan where they hydrolyze the glucosyl β -1,4 linkage, however to a lesser extent than the mannanases Cel45A and Man5A [34].

Conclusion

The data presented in this paper characterised the multicomponent carbohydrase system of a *T. reesei* secretome and demonstrated its strong cell wall degradation capacity as measured by viscosity reduction, and polysaccharide degradation through *in vitro* incubations and fluorescence and immunocytochemistry confocal microscopy visualization. It appears that the natural balance of carbohydrate-degrading enzymes found in the *T. reesei* secretome can hydrolyze the diverse and complex cell wall structures in monocot and dicot grains or grain by-products commonly used in the animal feed industry.

Supporting information

S1 Fig. Confocal images of cross sections of whole wheat grains labelled with the immunofluorescent probe LM28 detecting glucuronoarabinoxylans with high degree of branching.

The green colour indicates sample autofluorescence. Scale bar = 100 μ m.

(TIF)

S2 Fig. Confocal images of cross sections of whole barley grains labelled with the immunofluorescent probe LM28 detecting glucuronoarabinoxylans with high degree of branching.

The green colour indicates sample autofluorescence. Scale bar = 100 μ m.

(TIF)

S3 Fig. Confocal images of cross sections of whole oat grains. (A) Section of oat incubated with sodium acetate buffer (control) at pH 5 for 3 h and subsequently stained with Calcofluor White. (B) Similar sections of oat incubated with the carbohydrase product for 3 hours and stained with Calcofluor White. Scale bar = 50 μ m.

(TIF)

S4 Fig. Confocal images of cross sections of whole oat grains labelled with the immunofluorescent probe detecting β -glucans. (A) oat section incubated with sodium acetate buffer (control) at pH 5 for 3 h and subsequently incubated with the antibody detecting the β -glucans structures. (B) similar section of oat incubated with the carbohydrase product for 3 hours and then with the antibody detecting β -glucans and the secondary red-fluorescence labelled antibodies. Red colour indicates binding of the antibody to the β -glucans and the green colour indicates sample autofluorescence. Scale bar = 50 μ m.

(TIF)

S5 Fig. Confocal images of cross sections of DORB labelled with the immunofluorescent probe LM11 detecting arabinoxylans with low degree of branching. The green colour indicates sample autofluorescence. Scale bar = 100 μm .

(TIF)

S6 Fig. Confocal images of cross sections of whole rapeseed seeds labelled with the immunofluorescent probe LM25 detecting xyloglucans. The red colour indicates binding of the antibody to the xyloglucans and the green colour indicates sample autofluorescence. Scale bar = 100 μm .

(TIF)

S7 Fig. Confocal images of cross sections of whole rapeseed seeds labelled with the immunofluorescent probe LM6 detecting (1–5)- α -L-arabinans. The red colour indicates binding of the antibody to the arabinans and the green colour indicates sample autofluorescence. Scale bar = 50 μm .

(TIF)

S8 Fig. Confocal images of cross sections of whole cassava roots labelled with the immunofluorescent probe LM6 detecting (1–5)- α -L-arabinans. The red colour indicates binding of the antibody to the arabinans and the green colour indicates sample autofluorescence. Scale bar = 50 μm .

(TIF)

Acknowledgments

The authors acknowledge Peter Schimlér, Pernille Miller, Marinus Thinggaard Rostved and Jonas Ravn for help with the experimental work. The authors are also grateful to Tine Vitved Jensen, Adam Smith, Kostas Stamatopoulos, Nelson Ward and Jacqueline Sugitani Chimi-lovski de Souza for valuable discussions of the manuscript.

Author Contributions

Conceptualization: Ninfa Rangel Pedersen, Morten Tovborg, Eduardo Antonio Della Pia.

Data curation: Eduardo Antonio Della Pia.

Formal analysis: Eduardo Antonio Della Pia.

Investigation: Eduardo Antonio Della Pia.

Methodology: Eduardo Antonio Della Pia.

Project administration: Eduardo Antonio Della Pia.

Resources: Eduardo Antonio Della Pia.

Supervision: Ninfa Rangel Pedersen, Eduardo Antonio Della Pia.

Validation: Eduardo Antonio Della Pia.

Visualization: Morten Tovborg, Eduardo Antonio Della Pia.

Writing – original draft: Morten Tovborg, Abdoreza Soleimani Farjam, Eduardo Antonio Della Pia.

Writing – review & editing: Ninfa Rangel Pedersen, Morten Tovborg, Abdoreza Soleimani Farjam, Eduardo Antonio Della Pia.

References

1. William JB, Charles TA. Release, Recycle, Rebuild: Cell-Wall Remodeling, Autodegradation, and Sugar Salvage for New Wall Biosynthesis during Plant Development. *Molecular Plant*. 2018; 11(1):31–46. <https://doi.org/10.1016/j.molp.2017.08.011> PMID: 28859907
2. Rakszegi M, Lovegrove A, Balla K, Láng L, Bedő Z, Veisz O, et al. Effect of heat and drought stress on the structure and composition of arabinoxylan and β -glucan in wheat grain. *Carbohydr Polym*. 2014; 102:557–65. <https://doi.org/10.1016/j.carbpol.2013.12.005> PMID: 24507319
3. Jiali D. Isolation of a novel xyloglucan endotransglucosylase (OsXET9) gene from rice and analysis of the response of this gene to abiotic stresses. *African journal of biotechnology*. 2011; 10(76). <https://doi.org/10.5897/AJB11.1242>
4. Takahisa Hayashi Rumi K. Functions of Xyloglucan in Plant Cells. *Molecular Plant*. 2011; 4(1):17–24. <https://doi.org/10.1093/mp/ssq063> PMID: 20943810
5. Lee J, Nam DS, Kong C. Variability in nutrient composition of cereal grains from different origins. *Springerplus*. 2016; 5(1):1–6. <https://doi.org/10.1186/s40064-016-2046-3> PMID: 27099824
6. AB Vista. Reference guide: An introduction to Fibre Analysis using NIR 2020. Available from: <https://internationalfibre.com/reference-guides/>.
7. Global Feed Statistics: International Feed Industry Federation; 2020. Available from: <https://iff.org/global-feed/statistics/>.
8. Joaquin A, Paulino A. Carbohydrases are the Enzymes of the Future in Animal Feed2019. Available from: <https://en.engormix.com/poultry-industry/articles/carbohydrases-are-enzymes-future-t44657.htm>.
9. Gong W, Zhang H, Liu S, Zhang L, Gao P, Chen G, et al. Comparative Secretome Analysis of *Aspergillus niger*, *Trichoderma reesei*, and *Penicillium oxalicum* During Solid-State Fermentation. *Appl Biochem Biotechnol*. 2015; 177(6):1252–71. <https://doi.org/10.1007/s12010-015-1811-z> PMID: 26319683
10. Herpoël-Gimbert I, Margeot A, Dolla A, Jan G, Mollé D, Lignon S, et al. Comparative secretome analyses of two *Trichoderma reesei* RUT-C30 and CL847 hypersecretory strains. *Biotechnol Biofuels*. 2008; 1(1):18-. <https://doi.org/10.1186/1754-6834-1-18> PMID: 19105830
11. Ward N, Angel R, Levy A, Della Pia E, Tovborg M. A *Trichoderma reesei* enzyme tool-box generates soluble XOS from corn and improve performance of corn fed broilers. *International Poultry Scientific Forum [Internet]*. 2021. Available from: <https://www.researchgate.net/publication/349988645>.
12. Ward NE. Debranching enzymes in corn/soybean meal-based poultry feeds: a review. *Poultry Science*. 2021; 100(2):765–75. <https://doi.org/10.1016/j.psj.2020.10.074> PMID: 33518131
13. Villca B, Lizardo R, Broz J, Brufau J, Torrallardona D. Effect of a carbohydrase enzyme complex on the nutrient apparent total tract digestibility of rye-based diets fed to growing-finishing pigs under liquid feeding. *Journal of Animal Science*. 2016; 94(suppl_3):230–3. <https://doi.org/10.2527/jas.2015-9747>
14. Pedersen NR, Ravn JL, Pettersson D. A multienzyme NSP product solubilises and degrades NSP structures in canola and mediates protein solubilisation and degradation in vitro. *Animal Feed Science and Technology*. 2017; 234:244–52. <https://doi.org/10.1016/j.anifeedsci.2017.09.015>.
15. Abel GJ, Pettersson D, inventors; Novozymes A/S, assignee. Viscosity Pressure Assay2011.
16. Ravn JL, Martens HJ, Pettersson D, Pedersen NR. A commercial GH 11 xylanase mediates xylan solubilisation and degradation in wheat, rye and barley as demonstrated by microscopy techniques and wet chemistry methods. *Animal Feed Science and Technology*. 2016; 219:216–25. <https://doi.org/10.1016/j.anifeedsci.2016.06.020>.
17. Martinez D, Berka RM, Henrissat B, Saloheimo M, Arvas M, Baker SE, et al. Genome sequencing and analysis of the biomass-degrading fungus *Trichoderma reesei* (syn. *Hypocrea jecorina*). *Nature Biotechnology*. 2008; 26(5):553–60. <https://doi.org/10.1038/nbt1403> PMID: 18454138
18. Stals I, Samyn B, Sergeant K, White T, Hoorelbeke K, Coorevits A, et al. Identification of a gene coding for a deglycosylating enzyme in *Hypocrea jecorina*. *FEMS Microbiol Lett*. 2010; 303(1):9–17. <https://doi.org/10.1111/j.1574-6968.2009.01849.x> PMID: 20015338
19. He J, Yu B, Zhang K, Ding X, Chen D. Expression of endo-1, 4-beta-xylanase from *Trichoderma reesei* in *Pichia pastoris* and functional characterization of the produced enzyme. *BMC Biotechnol*. 2009; 9(1):56-. <https://doi.org/10.1186/1472-6750-9-56> PMID: 19527524
20. Biely P, Kremnický L, Alföldi J, Tenkanen M. Stereochemistry of the hydrolysis of glycosidic linkage by endo- β -1,4-xylanases of *Trichoderma reesei*. *FEBS Lett*. 1994; 356(1):137–40. [https://doi.org/10.1016/0014-5793\(94\)01248-2](https://doi.org/10.1016/0014-5793(94)01248-2) PMID: 7988708
21. Margolles-Clark E, Tenkanen M, Nakari-Setälä T, Penttilä M. Cloning of genes encoding alpha-L-arabinofuranosidase and beta-xylosidase from *Trichoderma reesei* by expression in *Saccharomyces cerevisiae*. *Appl Environ Microbiol*. 1996; 62(10):3840–6. <https://doi.org/10.1128/aem.62.10.3840-3846.1996> PMID: 8837440

22. Xu J, Takakuwa N, Nogawa M, Okada H, Morikawa Y. A third xylanase from *Trichoderma reesei* PC-3-7. *Applied microbiology and biotechnology*. 1998; 49(6):718–24. <https://doi.org/10.1007/s002530051237>
23. Margolles-Clark E, Tenkanen M, Soderlund H, Penttilä M. Acetyl Xylan Esterase from *Trichoderma reesei* Contains an Active-Site Serine Residue and a Cellulose-Binding Domain. *Eur J Biochem*. 1996; 237(3):553–60. <https://doi.org/10.1111/j.1432-1033.1996.0553p.x> PMID: 8647098
24. Gutiérrez R, Cederlund E, Hjelmqvist L, Peirano A, Herrera F, Ghosh D, et al. Acetyl xylan esterase II from *Penicillium purpurogenum* similar to an esterase from *Trichoderma reesei* but lacks a cellulose binding domain. *FEBS letters*. 1998; 423(1):35–8. [https://doi.org/10.1016/s0014-5793\(98\)00055-6](https://doi.org/10.1016/s0014-5793(98)00055-6) PMID: 9506837
25. Li X-L, Špániková S, de Vries RP, Biely P. Identification of genes encoding microbial glucuronoyl esterases. *FEBS Lett*. 2007; 581(21):4029–35. <https://doi.org/10.1016/j.febslet.2007.07.041> PMID: 17678650
26. Grishutin S, Gusakov A, Markov A, Ustinov B, Semenova M, Sinitsyn A. Specific xyloglucanases as a new class of polysaccharide-degrading enzymes. *Biochim Biophys Acta*. 2004; 1674(3):268–81. <https://doi.org/10.1016/j.bbagen.2004.07.001> PMID: 15541296
27. Gastebois A, Mouyna I, Simenel C, Clavaud C, Coddeville B, Delepierre M, et al. Characterization of a new beta(1–3)-glucan branching activity of *Aspergillus fumigatus*. *J Biol Chem*. 2010; 285(4):2386–96. <https://doi.org/10.1074/jbc.M109.077545> PMID: 19948732
28. da Silva Aires R, Steindorff AS, Ramada MHS, de Siqueira SJL, Ulhoa CJ. Biochemical characterization of a 27kDa 1,3-β-d-glucanase from *Trichoderma asperellum* induced by cell wall of *Rhizoctonia solani*. *Carbohydrate polymers*. 2012; 87(2):1219–23. <https://doi.org/10.1016/j.carbpol.2011.09.001>
29. Kuge T, Nagoya H, Tryfona T, Kurokawa T, Yoshimi Y, Dohmae N, et al. Action of an endo-β-1,3(4)-glucanase on cellobiosyl unit structure in barley β-1,3:1,4-glucan. *Biosci Biotechnol Biochem*. 2015; 79(11):1810–7. <https://doi.org/10.1080/09168451.2015.1046365> PMID: 26027730
30. Amandine G, Thierry F, Jean-Paul L, Isabelle M. β(1–3)Glucanosyltransferase Gel4p Is Essential for *Aspergillus fumigatus*. *Eukaryot Cell*. 2010; 9(8):1294–8. <https://doi.org/10.1128/EC.00107-10> PMID: 20543062
31. Fowler T, Brown JRD. The *bgl1* gene encoding extracellular beta-glucosidase from *Trichoderma reesei* is required for rapid induction of the cellulase complex. *Mol Microbiol*. 1992; 6(21):3225–35. <https://doi.org/10.1111/j.1365-2958.1992.tb01777.x> PMID: 1453960
32. Henrissat B, Driguez H, Viet C, Schülein M. Synergism of Cellulases from *Trichoderma reesei* in the Degradation of Cellulose. *Bio/technology* (New York, NY 1983). 1985; 3(8):722–6. <https://doi.org/10.1038/nbt0885-722>
33. Vincken J-P, Beldman G, Voragen AGJ. Substrate specificity of endoglucanases: what determines xyloglucanase activity? *Carbohydr Res*. 1997; 298(4):299–310. [https://doi.org/10.1016/s0008-6215\(96\)00325-4](https://doi.org/10.1016/s0008-6215(96)00325-4) PMID: 9098958
34. Karlsson J, Siika-aho M, Tenkanen M, Tjerneld F. Enzymatic properties of the low molecular mass endoglucanases Cel12A (EG III) and Cel45A (EG V) of *Trichoderma reesei*. *J Biotechnol*. 2002; 99(1):63–78. [https://doi.org/10.1016/s0168-1656\(02\)00156-6](https://doi.org/10.1016/s0168-1656(02)00156-6) PMID: 12204558
35. Arisan-Atac I, Hodits R, Kristufek D, Kubicek CP. Purification, and characterization of a β-mannanase of *Trichoderma reesei* C-30. *Applied microbiology and biotechnology*. 1993; 39(1):58–62. <https://doi.org/10.1007/BF00166849>
36. Margolles-Clark E, Tenkanen M, Luonteri E, Penttilä M. Three α-Galactosidase Genes of *Trichoderma reesei* Cloned by Expression in Yeast. *European Journal of Biochemistry*. 1996; 240:104–11. <https://doi.org/10.1111/j.1432-1033.1996.0104h.x> PMID: 8797842
37. Jääskeläinen A-S, Holopainen-Mantila U, Tamminen T, Vuorinen T. Endosperm and aleurone cell structure in barley and wheat as studied by optical and Raman microscopy. *Journal of cereal science*. 2013; 57(3):543–50. <https://doi.org/10.1016/j.jcs.2013.02.007>
38. Anderson CT, Carroll A, Akhmetova L, Somerville C. Real-Time Imaging of Cellulose Reorientation during Cell Wall Expansion in *Arabidopsis* Roots. *Plant Physiology*. 2010; 152(2):787. <https://doi.org/10.1104/pp.109.150128> PMID: 19965966
39. Chowdhury J, Henderson M, Schweizer P, Burton RA, Fincher GB, Little A. Differential accumulation of callose, arabinoxylan and cellulose in nonpenetrated versus penetrated papillae on leaves of barley infected with *Blumeria graminis* f. sp. *hordei*. *New Phytologist*. 2014; 204(3):650–60. <https://doi.org/10.1111/nph.12974> PMID: 25138067
40. Perez-Ternero C, Macià A, de Sotomayor MA, Parrado J, Motilva M-J, Herrera M-D. Bioavailability of the ferulic acid-derived phenolic compounds of a rice bran enzymatic extract and their activity against superoxide production. *Food Funct*. 2017; 8(6):2165–74. <https://doi.org/10.1039/c7fo00243b> PMID: 28524914

41. Lynd LR, Weimer PJ, van Zyl WH, Pretorius IS. Microbial Cellulose Utilization: Fundamentals and Biotechnology. *Microbiol Mol Biol Rev.* 2002; 66(3):506–77. <https://doi.org/10.1128/MMBR.66.3.506-577.2002> PMID: 12209002
42. Lehmann L, Rønnest NP, Jørgensen CI, Olsson L, Stocks SM, Jørgensen HS, et al. Linking hydrolysis performance to *Trichoderma reesei* cellulolytic enzyme profile. *Biotechnol Bioeng.* 2016; 113(5):1001–10. <https://doi.org/10.1002/bit.25871> PMID: 26524197
43. Häkkinen M, Arvas M, Oja M, Aro N, Penttilä M, Saloheimo M, et al. Re-annotation of the CAZy genes of *Trichoderma reesei* and transcription in the presence of lignocellulosic substrates. *Microb Cell Fact.* 2012; 11(1):134–. <https://doi.org/10.1186/1475-2859-11-134> PMID: 23035824
44. Tenkanen M, Vršanská M, Siika-aho M, Wong DW, Puchart V, Penttilä M, et al. Xylanase XYN IV from *Trichoderma reesei* showing exo- and endo-xylanase activity. *FEBS J.* 2013; 280(1):285–301. <https://doi.org/10.1111/febs.12069> PMID: 23167779
45. Monrad RN, Eklöf J, Krogh KBRM, Biely P. Glucuronoyl esterases: diversity, properties and biotechnological potential. A review. *Critical Reviews in Biotechnology.* 2018; 38(7):1121–36. <https://doi.org/10.1080/07388551.2018.1468316> PMID: 29739247
46. Ravn JL, Gliitsø V, Pettersson D, Ducatelle R, Van Immerseel F, Pedersen NR. Combined endo- β -1,4-xylanase and α -l-arabinofuranosidase increases butyrate concentration during broiler cecal fermentation of maize glucurono-arabinoxylan. *Animal Feed Science and Technology.* 2018; 236:159–69. <https://doi.org/10.1016/j.anifeedsci.2017.12.012>.
47. Im HL, Ravindran V, Ravindran G, Pittolo PH, Bryden WL. The apparent metabolisable energy and amino acid digestibility of wheat, triticale and wheat middlings for broiler chickens as affected by exogenous xylanase supplementation. *Journal of the science of food and agriculture.* 1999; 79(12):1727–32. [https://doi.org/10.1002/\(SICI\)1097-0010\(199909\)79:12<1727::AID-JSFA428>3.0.CO;2-K](https://doi.org/10.1002/(SICI)1097-0010(199909)79:12<1727::AID-JSFA428>3.0.CO;2-K)
48. Austin SC, Wiseman J, Chesson A. Influence of Non-Starch Polysaccharides Structure on the Metabolizable Energy of U.K. Wheat Fed to Poultry. *Journal of cereal science.* 1999; 29(1):77–88. <https://doi.org/10.1006/jcrs.1998.0213>
49. Pettersson D, Graham H, Åman P. The nutritive value for broiler chickens of pelleting and enzyme supplementation of a diet containing barley, wheat and rye. *Animal feed science and technology.* 1991; 33(1):1–14. [https://doi.org/10.1016/0377-8401\(91\)90041-P](https://doi.org/10.1016/0377-8401(91)90041-P)
50. Masey O'Neill HV, Smith JA, Bedford MR. Multicarbohydrase Enzymes for Non-ruminants. *Asian-Australas J Anim Sci.* 2014; 27(2):290–301. <https://doi.org/10.5713/ajas.2013.13261> PMID: 25049954
51. Bacic A, Stone B. A (1 \rightarrow 3)- and (1 \rightarrow 4)-linked β -d-glucan in the endosperm cell-walls of wheat. *Carbohydrate research.* 1980; 82(2):372–7. [https://doi.org/10.1016/S0008-6215\(00\)85713-4](https://doi.org/10.1016/S0008-6215(00)85713-4)
52. Meikle PJ, Hoogenraad NJ, Bonig I, Clarke AE, Stone BA. A 1,3/1,4-beta-glucan-specific monoclonal antibody and its use in the quantitation and immunocytochemical location of 1,3/1,4-beta-glucans. *Plant J.* 1994; 5(1):1–9. <https://doi.org/10.1046/j.1365-313x.1994.5010001.x> PMID: 8130794
53. Fernandes VO, Costa M, Ribeiro T, Serrano L, Cardoso V, Santos H, et al. 1,3–1,4- β -Glucanases and not 1,4- β -glucanases improve the nutritive value of barley-based diets for broilers. *Animal feed science and technology.* 2016; 211:153–63. <https://doi.org/10.1016/j.anifeedsci.2015.11.007>
54. Brenes A, Smith M, Guenter W, Marquardt RR. Effect of enzyme supplementation on the performance and digestive tract size of broiler chickens fed wheat- and barley-based diets. *Poult Sci.* 1993; 72(9):1731–9. <https://doi.org/10.3382/ps.0721731> PMID: 8234133
55. Müller G, Chylenski P, Bissaro B, Eijnsink VGH, Horn SJ. The impact of hydrogen peroxide supply on LPMO activity and overall saccharification efficiency of a commercial cellulase cocktail. *Biotechnology for Biofuels.* 2018; 11(1):209. <https://doi.org/10.1186/s13068-018-1199-4> PMID: 30061931
56. Guais O, Tourrasse O, Dourdoigne M, Parrou JL, Francois JM. Characterization of the family GH54 α -l-arabinofuranosidases in *Penicillium funiculosum*, including a novel protein bearing a cellulose-binding domain. *Appl Microbiol Biotechnol.* 2010; 87(3):1007–21. <https://doi.org/10.1007/s00253-010-2532-4> PMID: 20333513
57. Willats WGT, Marcus SE, Knox JP. Generation of a monoclonal antibody specific to (1 \rightarrow 5)- α -l-arabinan. *Carbohydr Res.* 1998; 308(1–2):149–52. [https://doi.org/10.1016/S0008-6215\(98\)00070-6](https://doi.org/10.1016/S0008-6215(98)00070-6) PMID: 9675359
58. Seiboth B, Metz B. Fungal arabinan and l-arabinose metabolism. *Appl Microbiol Biotechnol.* 2011; 89(6):1665–73. <https://doi.org/10.1007/s00253-010-3071-8> PMID: 21212945
59. Burton RA, Fincher GB. Evolution and development of cell walls in cereal grains. *Front Plant Sci.* 2014; 5:456–. <https://doi.org/10.3389/fpls.2014.00456> PMID: 25309555
60. Gigli-Bisceglia N, Engelsdorf T, Hamann T. Plant cell wall integrity maintenance in model plants and crop species-relevant cell wall components and underlying guiding principles. *Cell Mol Life Sci.* 2019; 77(11):2049–77. <https://doi.org/10.1007/s00018-019-03388-8> PMID: 31781810

61. Ravn JL, Martens HJ, Pettersson D, Pedersen NR. Enzymatic Solubilisation and Degradation of Soybean Fibre Demonstrated by Viscosity, Fibre Analysis and Microscopy. *Journal of agricultural science (Toronto)*. 2015; 7(9). <https://doi.org/10.5539/jas.v7n9p1>
62. Kyu MT, Dar B, Aye SS, Matsuda T. Prebiotic Oligosaccharides Prepared by Enzymatic Degradation of Dietary Fibers in Rice Grains. *Journal of nutritional science and vitaminology*. 2019; 65(Supplement): S143–S7. <https://doi.org/10.3177/jnsv.65.S143> PMID: 31619616
63. Schultink A, Liu L, Zhu L, Pauly M. Structural Diversity and Function of Xyloglucan Sidechain Substituents. *Plants (Basel)*. 2014; 3(4):526–42. <https://doi.org/10.3390/plants3040526> PMID: 27135518
64. Arnal G, Stogios PJ, Asohan J, Attia MA, Skarina T, Viborg AH, et al. Substrate specificity, regiospecificity, and processivity in glycoside hydrolase family 74. *J Biol Chem*. 2019; 294(36):13233–47. <https://doi.org/10.1074/jbc.RA119.009861> PMID: 31324716
65. Desmet T, Cantaert T, Gualfetti P, Nerinckx W, Gross L, Mitchinson C, et al. An investigation of the substrate specificity of the xyloglucanase Cel74A from *Hypocrea jecorina*. *FEBS J*. 2007; 274(2):356–63. <https://doi.org/10.1111/j.1742-4658.2006.05582.x> PMID: 17229143
66. Sinitsyna OA, Fedorova EA, Pravilnikov AG, Rozhkova AM, Skomarovsky AA, Matys VY, et al. Isolation and properties of xyloglucanases of *Penicillium* sp. *Biochemistry (Mosc)*. 2010; 75(1):41–9. <https://doi.org/10.1134/s0006297910010062> PMID: 20331423
67. Glamocic D, Polovinski-Horvatovic M, Ivkovic M, Beukovic D, Bjedov S. Effects of enzymes supplementation on digestibility and energy utilizations of broilers diets with different metabolizable energy level. *Biotechnology in Animal Husbandry*. 2011; 27(3):583–90. <https://doi.org/10.2298/BAH1103583G>
68. Oladunjoye I, Ojebiyi O. Performance characteristics of broiler chicken (*Gallus gallus*) fed rice (*Oryza sativa*) bran with or without roxazyme G2G. *Int J Anim Vet Adv*. 2010; 2(4):5.
69. Hsiao HY, Anderson DM, Dale NM. Levels of β -Mannan in Soybean Meal. *Poult Sci*. 2006; 85(8):1430–2. <https://doi.org/10.1093/ps/85.8.1430> PMID: 16903473
70. Stålbrand H, Siika-aho M, Tenkanen M, Viikari L. Purification and characterization of two β -mannanases from *Trichoderma reesei*. *Journal of biotechnology*. 1993; 29(3):229–42. [https://doi.org/10.1016/0168-1656\(93\)90055-r](https://doi.org/10.1016/0168-1656(93)90055-r)